Admittance Control using a Base Force/Torque Sensor. ⋆

Christian Ott and Yoshihiko Nakamura

Department of Mechano-Informatics, University of Tokyo, Japan
(e-mail: {ott,nakamura}@ynl.t.u-tokyo.ac.jp).

Abstract: In this paper we investigate on the use of a base force/torque sensor for implementing position based impedance control (i.e. admittance control). By utilizing measurements of the contact force at the base of a robot manipulator, it is possible to perceive forces acting all along the robot's structure. This can be used for implementing a compliant motion control algorithm which is not limited to physical interaction at the end-effector only. We show that the use of a base force sensor instead of a sensor mounted on the end-effector poses certain limitations on the achievable closed loop dynamics. The stability and passivity properties are exemplified by an analysis for the one-degree-of-freedom case. The control performance in the multi-degrees-of-freedom case is verified by a simulation study of a Cartesian admittance controller.

Keywords: Robot control, Admittance control, Impedance control, Compliance control, Force Feedback, Base force/torque sensor

1. INTRODUCTION

Impedance and compliance control for rigid-body manipulators are a mature field of robotics studied for more than twenty years [1]. For implementing classical impedance control (with impedance causality) a precise torque control interface is imperative. While this can be made possible with some effort by equipping the robot with torque sensors and using an inner loop torque control [2–4], many commercial robots still do not provide a torque control interface. In such a case, a compliant impedance behavior can be imposed by admittance control [1] via additional measurement of the external forces using a force/torque sensor (FTS) mounted at the end-effector [5]. In this case, the compliant behavior clearly can be achieved only with respect to forces acting on the tip of the robot, where they are perceived by the FTS. All other forces acting along the robot's structure are not considered. This shortcoming of FTS based compliance control lead to the development of force sensitive skins [6] and whole body joint torque sensing [7,8].

In this paper, we propose an alternative solution to classical admittance control by replacing the FTS at the end-effector by a FTS mounted at the robot's base. Thereby, it becomes possible to perceive forces all along the robot's structure independently of joint friction. Having mounted the FTS at the base, the question arises to what extent one still can implement a desired impedance behavior since the base mounted FTS will also measure all (static and) dynamic forces of the controlled manipulator. Apart from applications to fixed mounted manipulators, we expect that the same issue can also be relevant for implementing whole body impedance controllers of humanoid robots based on the feet force sensors, which often are applied for controlling the interaction forces of the robot with the ground during walking [9].

The use of base mounted FTSs for identification and joint torque estimation has been well studied in the works of Dubowsky et al. [10–12]. In [11], a method for estimating the dynamical parameters of a serial manipulator arm was presented. Due to the measurement of the base force, no joint torque information was required in the identification procedure. In [12], the base FTS was used for estimating the robot's joint torques based on known dynamical parameters. The estimated torque signal was used for implementing an inner torque control loop, which was augmented by an outer PD position controller.

In contrast to [12], we aim at incorporating the base force measurement directly into the design of an admittance controller instead of implementing an inner loop torque controller. Therefore, the desired impedance relation will be transformed into a dynamic relation between the contact force at the base and the robot's motion. We will highlight some restrictions on the achievable closed loop dynamics which are due to the dislocation of the force sensing. The controller design is motivated by the simplified situation of a one-degree-of-freedom (one-DOF) model for which a stability analysis is given.

2. MODELING

Since the contact force at the base is an internal force, it usually is not represented in the equations of motion of a multi-body robot manipulator. For deriving an expression of the base force, we therefore start with a more complicated model of a free-floating robot manipulator (Fig. 1). All motion of the base body will be restricted by adding kinematical constraints such that the system

⋆ This research is partly supported by Special Coordination Funds for Promoting Science and Technology, "IRT Foundation to Support Man and Aging Society".

[1] also referred to as *position based impedance control*

renders the dynamics of a fixed-base manipulator. In this way, the Lagrangian multipliers related to the constraints will represent the measured base force [13].

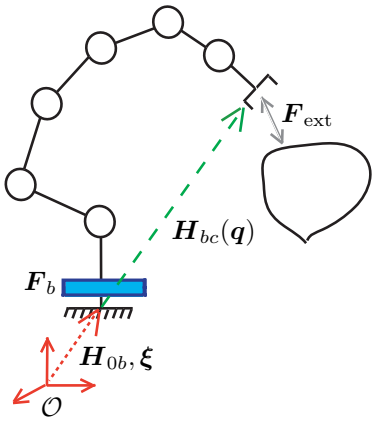

Fig. 1. Model of a robot manipulator mounted on a base FTS. The fixed base manipulator model is augmented by a free-floating base link, for which the motion will be constrained.

Let $\boldsymbol{H}_{0b} \in SE(3)$ be the homogeneous transformation describing the position and orientation of the robot's base link and $\boldsymbol{\xi} \in se(3)$ be the associated body twist [14]. The n joint angles and the joint torques of the robot are given by $\boldsymbol{q} \in \mathbb{R}^n$ and $\boldsymbol{\tau} \in \mathbb{R}^n$, respectively. The considered free-floating robot dynamics can then be written as

$$\bar{\boldsymbol{M}}(\boldsymbol{q}) \begin{pmatrix} \dot{\boldsymbol{\xi}} \\ \ddot{\boldsymbol{q}} \end{pmatrix} + \bar{\boldsymbol{C}}(\boldsymbol{q}, \dot{\boldsymbol{q}}, \boldsymbol{\xi}) \begin{pmatrix} \boldsymbol{\xi} \\ \dot{\boldsymbol{q}} \end{pmatrix} + \bar{\boldsymbol{g}}(\boldsymbol{q}, \boldsymbol{H}_{0b}) = \begin{pmatrix} \boldsymbol{0} \\ \boldsymbol{\tau} \end{pmatrix} - \begin{pmatrix} \boldsymbol{F}_b \\ \boldsymbol{0} \end{pmatrix} + \boldsymbol{\tau}_{\text{ext}} \ , \tag{1}$$

wherein $\bar{\boldsymbol{M}}(\boldsymbol{q}) \in \mathbb{R}^{(6+n)\times(6+n)}$ denotes the complete inertia matrix including the base link [13]. The centrifugal and Coriolis terms are given via the matrix $\bar{\boldsymbol{C}}(\boldsymbol{q}, \dot{\boldsymbol{q}}, \boldsymbol{\xi})$. The gravity term is written as $\bar{\boldsymbol{g}}(\boldsymbol{q}, \boldsymbol{H}_{0b}) \in \mathbb{R}^{(6+n)}$. The wrench $\boldsymbol{F}_b \in se^*(3)$ represents the generalized base force measured by the FTS. The generalized external forces (except for the generalized forces $\boldsymbol{F}_b$ exerted at the base at the location of the FTS) acting on the robot are summarized by the vector $\boldsymbol{\tau}_{\text{ext}}$. In case that the external torques are due to a wrench $\boldsymbol{F}_{\text{ext}} \in se^*(3)$ acting at the end-effector, they are given by

$$\boldsymbol{\tau}_{\text{ext}} = \begin{pmatrix} \boldsymbol{\tau}_{\text{ext,b}} \\ \boldsymbol{\tau}_{\text{ext,m}} \end{pmatrix} = \begin{bmatrix} \boldsymbol{Ad}_{H_{bc}}^{-T}(\boldsymbol{q}) \\ \boldsymbol{J}_{bc}^{T}(\boldsymbol{q}) \end{bmatrix} \boldsymbol{F}_{\text{ext}} \ , \tag{2}$$

with $\boldsymbol{Ad}_{H_{bc}}(\boldsymbol{q}) \in \mathbb{R}^{(6\times6)}$ as the adjoint for the homogeneous transformation $\boldsymbol{H}_{bc}(\boldsymbol{q}) \in SE(3)$ between the base frame and the end-effector frame, and $\boldsymbol{J}_{bc}(\boldsymbol{q}) \in \mathbb{R}^{6\times n}$ as the corresponding body Jacobian [14].

Since we are considering a fixed base manipulator, the dynamics (1) is subjected to the constraint

$$\dot{\boldsymbol{H}}_{0b} = \boldsymbol{0} \Rightarrow \underbrace{[\boldsymbol{I} \ \boldsymbol{0}]}_{\boldsymbol{\Phi}} \begin{pmatrix} \boldsymbol{\xi} \\ \dot{\boldsymbol{q}} \end{pmatrix} = \boldsymbol{0} \ , \tag{3}$$

such that the base force $\boldsymbol{F}_b$ represents the Lagrangian multipliers according to the constraint (3). In the following, we will derive three different relations from (1) and (3):

(A) The robot dynamics, which defines a relation $\ddot{\boldsymbol{q}} \rightleftharpoons \boldsymbol{\tau}$.
(B) A relation $\boldsymbol{F}_b \rightleftharpoons \ddot{\boldsymbol{q}}$.
(C) A relation $\boldsymbol{F}_b \rightleftharpoons \boldsymbol{\tau}$.

Due to the constraint (3), we can set $\boldsymbol{\xi} = \boldsymbol{0}$ as well as $\dot{\boldsymbol{\xi}} = \boldsymbol{0}$, and consequently drop the dependence of the gravity term on the constant frame $\boldsymbol{H}_{0b}$. Also, let us rewrite $\bar{\boldsymbol{M}}(\boldsymbol{q})$, $\bar{\boldsymbol{C}}(\boldsymbol{q}, \dot{\boldsymbol{q}}, \boldsymbol{0})$, and $\bar{\boldsymbol{g}}(\boldsymbol{q}, \boldsymbol{H}_{0b})$ in the form

$$\bar{\boldsymbol{M}}(\boldsymbol{q}) = \begin{bmatrix} \boldsymbol{M}_b(\boldsymbol{q}) & \boldsymbol{M}_c(\boldsymbol{q}) \\ \boldsymbol{M}_c^T(\boldsymbol{q}) & \boldsymbol{M}(\boldsymbol{q}) \end{bmatrix}, \quad \bar{\boldsymbol{g}}(\boldsymbol{q}, \boldsymbol{H}_{0b}) = \begin{pmatrix} \boldsymbol{g}_b(\boldsymbol{q}) \\ \boldsymbol{g}(\boldsymbol{q}) \end{pmatrix} \ ,$$
$$\bar{\boldsymbol{C}}(\boldsymbol{q}, \dot{\boldsymbol{q}}, \boldsymbol{0}) = \begin{bmatrix} \boldsymbol{C}_b(\boldsymbol{q}, \dot{\boldsymbol{q}}) & \boldsymbol{C}_1(\boldsymbol{q}, \dot{\boldsymbol{q}}) \\ \boldsymbol{C}_2(\boldsymbol{q}, \dot{\boldsymbol{q}}) & \boldsymbol{C}(\boldsymbol{q}, \dot{\boldsymbol{q}}) \end{bmatrix} \ ,$$

where $\boldsymbol{M}(\boldsymbol{q}) \in \mathbb{R}^{n\times n}$ is the joint level inertia matrix and $\boldsymbol{M}_c(\boldsymbol{q}) \in \mathbb{R}^{(6\times n)}$ represents the inertia coupling matrix between the manipulator and the base link.

The relation (A) can be found if one pre-multiplies (1) by a matrix spanning the left nullspace of $\boldsymbol{\Phi}^T$, i.e. by $[\boldsymbol{0} \ \boldsymbol{I}]$. This results in the conventional rigid-body robot dynamics

$$\boldsymbol{M}(\boldsymbol{q})\ddot{\boldsymbol{q}} + \boldsymbol{C}(\boldsymbol{q}, \dot{\boldsymbol{q}})\dot{\boldsymbol{q}} + \boldsymbol{g}(\boldsymbol{q}) = \boldsymbol{\tau} + \boldsymbol{\tau}_{\text{ext,m}} \ . \tag{4}$$

Utilizing the property $\boldsymbol{\Phi}[\boldsymbol{0} \ \boldsymbol{I}]^T = \boldsymbol{0}$, relation (B) is obtained if (1) is pre-multiplied by $\boldsymbol{\Phi}$, which leads to

$$\boldsymbol{F}_b = \boldsymbol{\tau}_{\text{ext,b}} - \boldsymbol{M}_c(\boldsymbol{q})\ddot{\boldsymbol{q}} - \boldsymbol{C}_1(\boldsymbol{q}, \dot{\boldsymbol{q}})\dot{\boldsymbol{q}} - \boldsymbol{g}_b(\boldsymbol{q}) \ . \tag{5}$$

Finally, relation (C) can be obtained as follows. First, one computes the time derivative of the constraint equation (3) and substitutes the accelerations from (1) by inverting $\bar{\boldsymbol{M}}(\boldsymbol{q})$. By solving the resulting equation for $\boldsymbol{F}_b$, one gets

$$\boldsymbol{F}_b = \boldsymbol{\Phi}^{M+}(\boldsymbol{q}) \left(\boldsymbol{\tau}_{\text{ext}} + \begin{pmatrix} \boldsymbol{0} \\ \boldsymbol{\tau} \end{pmatrix} - \begin{bmatrix} \boldsymbol{C}_1(\boldsymbol{q}, \dot{\boldsymbol{q}})\dot{\boldsymbol{q}} + \boldsymbol{g}_b(\boldsymbol{q}) \\ \boldsymbol{C}(\boldsymbol{q}, \dot{\boldsymbol{q}})\dot{\boldsymbol{q}} + \boldsymbol{g}(\boldsymbol{q}) \end{bmatrix} \right) , \tag{6}$$

where the matrix $\boldsymbol{\Phi}^{M+}(\boldsymbol{q})$ is given by

$$\boldsymbol{\Phi}^{M+}(\boldsymbol{q}) := (\boldsymbol{\Phi}\bar{\boldsymbol{M}}^{-1}(\boldsymbol{q})\boldsymbol{\Phi}^T)^{-1}\boldsymbol{\Phi}\bar{\boldsymbol{M}}^{-1}(\boldsymbol{q}) \ .$$

Moreover, it can be shown that the matrix $\boldsymbol{\Phi}^{M+}$ is given by $\boldsymbol{\Phi}^{M+} = \begin{bmatrix} \boldsymbol{I} & -\boldsymbol{M}_c(\boldsymbol{q})\boldsymbol{M}^{-1}(\boldsymbol{q}) \end{bmatrix}$ (see Appendix A).

The above three relations between $\ddot{\boldsymbol{q}}$, $\boldsymbol{\tau}$, and $\boldsymbol{F}_b$ as presented in (4)-(6) will be relevant for the derivation and analysis of the admittance controller in the next sections. From (6) and (5) it becomes clear that the base force measured by the FTS depends not only on the robot's state $(\boldsymbol{q}, \dot{\boldsymbol{q}})$ and the generalized external forces $\boldsymbol{\tau}_{\text{ext}}$, but also on the current joint torque $\boldsymbol{\tau}$, which is considered as the control input in our case. It should be mentioned that therefore the use of this force in the controller is from a theoretical point of view not unproblematic. This issue basically arises because we ignore the force sensor's elasticity in the model and treat it as an ideal force sensing element. However, in any case we should avoid direct feedback from the force sensor measurement to the joint torque output of the controller as this feedback would be ill-defined.

3. ADMITTANCE CONTROL: ONE-DOF CASE

In this section, we take a simple one-DOF model as an example for the design of the admittance controller. The

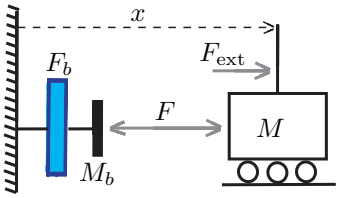

Fig. 2. Model of single mass, actuated by the force F and mounted on a base force sensor.

extension to the multi-body case will be treated in the next section.

Figure 2 shows the considered model. The position of the mass M is denoted by x. The control input is given by the actuator force F, which is acting in between the mass and the base. The external force is denoted by F_{ext}. With regard to the model described in Section 2, we have the following correspondences: $\boldsymbol{q} \hat{=} x$, $\boldsymbol{\tau} \hat{=} F$, $\boldsymbol{\tau}_{\text{ext,b}} \hat{=} F_{\text{ext}}$, and $\boldsymbol{\tau}_{\text{ext,m}} \hat{=} F_{\text{ext}}$.

It can easily be verified that in this simple case the coupling matrix $\boldsymbol{M}_c(\boldsymbol{q})$ is given by M and thus the complete inertia matrix becomes

$$\bar{\boldsymbol{M}} = \begin{bmatrix} M_b + M & M \\ M & M \end{bmatrix} .$$

Consequently, $\boldsymbol{\Phi}^{M+}$ is simply given by $\boldsymbol{\Phi}^{M+} = [1 \quad -1]$. The equations (4)-(6) are given by

$$\text{(A)} \quad M\ddot{x} = F + F_{\text{ext}} , \tag{7}$$

$$\text{(B)} \quad F_b = F_{\text{ext}} - M\ddot{x} , \tag{8}$$

$$\text{(C)} \quad F_b = -F , \tag{9}$$

as can also be easily verified by direct observation from Fig. 2. In particular (9) has a very simple form for this case, since the measured base force is here just the reaction force of the actuator force F.

As a desired impedance, we assume a relation $\Im(\dot{x}, F_{\text{ext}})$ of the form

$$\Im(\dot{x}, F_{\text{ext}}) : \; M_d\ddot{x} + D_d\dot{x} + K_d(x - x_0) = F_{\text{ext}} , \tag{10}$$

with $M_d > 0$, $D_d > 0$, and $K_d > 0$ as the desired inertia, damping, and stiffness, respectively. Herein $x_0 \in \mathbb{R}$ is the virtual equilibrium position. Equation (10) is a relation $\Im(\dot{x}, F_{\text{ext}})$ between $\dot{x}$ and the external force. In order to convert this relation into a relation $\Im^*(\dot{x}, F_b)$ between $\dot{x}$ and the base force ($\Im(\dot{x}, F_{\text{ext}}) \Rightarrow \Im^*(\dot{x}, F_b)$), we utilize (8) to get

$$\Im^*(\dot{x}, F_b) : \; (M_d - M)\ddot{x} + D_d\dot{x} + K_d(x - x_0) = F_b . \tag{11}$$

From (11) we see that the target inertia must always be larger than M, otherwise (11) would result in an unstable dynamics. Our strategy for the controller design is now to implement relation (11) via admittance control, i.e. by using an underlying position controller. If we assume an ideal position controller, the position x and the desired position x_d commanded to the position controller would be identical $x \to x_d$. Therefore, we replace x in (11) by x_d and augment it by a position controller (Fig. 3).

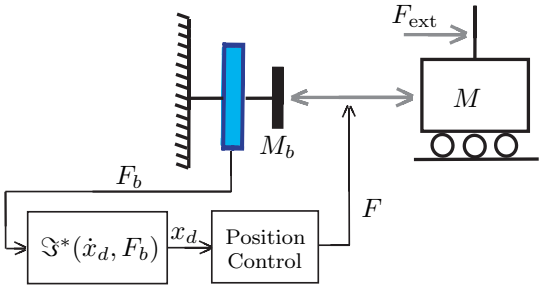

Fig. 3. Admittance control of the one-DOF model using a FTS at the base.

In order to analyze the stability of the resulting closed loop system, we have to assume a position control law. Using a simple PD controller of the form

$$F = -P(x - x_d) - D(\dot{x} - \dot{x}_d) , \tag{12}$$

with positive proportional and derivative gains $P > 0$ and $D > 0$, we get the following closed loop system

$$M\ddot{x} = -P(x - x_d) - D(\dot{x} - \dot{x}_d) + F_{\text{ext}} ,$$
$$(M_d - M)\ddot{x}_d + D_d\dot{x}_d + K_d(x_d - x_0) = F_b .$$

The base force can be removed from this equations by utilizing (9) and (12), such that we finally obtain

$$M\ddot{x} + D(\dot{x} - \dot{x}_d) + P(x - x_d) = F_{\text{ext}} , \tag{13}$$

$$(M_d - M)\ddot{x}_d + D_d\dot{x}_d + K_d(x_d - x_0) = P(x - x_d) + D(\dot{x} - \dot{x}_d) . \tag{14}$$

Since the impedance relation (11) and the PD control law (12) allow for a simple physical interpretation, we can perform the stability analysis based on energy considerations. This leads to the "energy" function

$$V(x, x_d, \dot{x}, \dot{x}_d) = \frac{1}{2}M\dot{x}^2 + \frac{1}{2}(M_d - M)\dot{x}_d^2 + \frac{1}{2}P(x - x_d)^2 + \frac{1}{2}K_d(x_d - x_0)^2 ,$$

which is positive definite if the condition $M_d > M$ holds. It is straightforward to show that the time derivative of this function along the solutions of (13)-(14) is given by

$$\dot{V}(x, x_d, \dot{x}, \dot{x}_d) = -D_d\dot{x}_d^2 - D(\dot{x} - \dot{x}_d)^2 + \dot{x}F_{\text{ext}} .$$

From this, one can immediately conclude that the system is passive with respect to the input F_{ext} and the output $\dot{x}$. Moreover, for the case of free motion, i.e. for $F_{\text{ext}} = 0$, the equilibrium point $x = x_d = x_0$ is stable in the sense of Lyapunov. By a closer analysis based on La'Salle's invariance principle, one can, furthermore, show that the system is asymptotically stable. Clearly, since the closed loop system (13)-(14) of the simple one-DOF case is linear, this can be shown also by a standard linear analysis.

4. EXTENSION TO CARTESIAN ADMITTANCE CONTROL OF A MULTI-BODY ROBOT

From (11) one can see that for the one-DOF case only impedance relations with a desired inertia M_d larger than

M can be realized. The reason for this is that the force measurement at the base is affected by the dynamics of the manipulator. In this section we will analyze the situation for a multi-body robot by following the design idea from the simple one-DOF case. In particular, we are aiming at the design of a Cartesian admittance controller. Notice that, if the one-DOF mass from Fig. 2 is replaced by a 6-DOF rigid-body, the analysis from the previous section can be applied without modification.

The desired impedance behavior shall be defined in Cartesian coordinates $\boldsymbol{x} = \boldsymbol{f}(\boldsymbol{q}) \in \mathbb{R}^6$, $\dot{\boldsymbol{x}} = \boldsymbol{J}(\boldsymbol{q})\dot{\boldsymbol{q}}$, where $\boldsymbol{f}(\boldsymbol{q})$ represents the forward kinematic mapping and $\boldsymbol{J}(\boldsymbol{q}) \in \mathbb{R}^{(6\times 6)}$ the analytic Jacobian $\boldsymbol{J}(\boldsymbol{q}) := \partial \boldsymbol{f}(\boldsymbol{q})/\partial \boldsymbol{q}$. In the following derivations, we will consider the non-redundant case and assume that the Jacobian is non-singular (and thus invertible) in the relevant workspace. Extensions to the redundant case would additionally require to consider the effect of the nullspace dynamics (see, e.g., [15,16]) on the measurement of the base FTS.

Similar to Sec. 3, we assume a desired impedance $\Im(\dot{\boldsymbol{x}}, \boldsymbol{F}_{\text{ext,c}})$ in form of a mass-spring-damper-like system

$$\Im(\dot{\boldsymbol{x}}, \boldsymbol{F}_{\text{ext,c}}): \ \boldsymbol{\Lambda}_d \ddot{\boldsymbol{x}} + \boldsymbol{D}_d \dot{\boldsymbol{x}} + \boldsymbol{K}_d(\boldsymbol{x} - \boldsymbol{x}_d) = \boldsymbol{F}_{\text{ext,c}} \ , \quad (15)$$

with the symmetric and positive definite matrices $\boldsymbol{\Lambda}_d \in \mathbb{R}^{6\times 6}$, $\boldsymbol{D}_d \in \mathbb{R}^{6\times 6}$, and $\boldsymbol{K}_d \in \mathbb{R}^{6\times 6}$ representing the desired inertia, damping, and stiffness, respectively. The virtual equilibrium position is given by $\boldsymbol{x}_d \in \mathbb{R}^6$. The external generalized forces are represented in (15) by the vector $\boldsymbol{F}_{\text{ext,c}}$, which is related to the external joint torques acting on the manipulator via $\boldsymbol{J}^T(\boldsymbol{q})\boldsymbol{F}_{\text{ext,c}} = \boldsymbol{\tau}_{\text{ext,m}}$.

Using (2), one can see that, if external forces are only exerted at the tip via the external wrench $\boldsymbol{F}_{\text{ext}}$ and no other external forces are acting, the external generalized forces at the base link are given by

$$\boldsymbol{\tau}_{\text{ext,b}} = \underbrace{\boldsymbol{Ad}_{H_{bc}}^{-T}(\boldsymbol{q})\boldsymbol{J}_{bc}^{-T}(\boldsymbol{q})\boldsymbol{J}^T(\boldsymbol{q})}_{\boldsymbol{J}_b^T(\boldsymbol{q})} \boldsymbol{F}_{\text{ext,c}} \ . \quad (16)$$

While in (15) we assume an expected point of contact $\boldsymbol{f}(\boldsymbol{q})$ at the robot's end-effector at which the desired impedance behavior is specified, the feedback of the generalized forces measured at the base will result in a reactive compliant impedance behavior even if the external forces are not exerted exactly at the end-effector but somewhere else on the robot. Clearly, for forces exerted in the vicinity of the end-effector, the perceived impedance will be close to (15). On the other hand, if the external forces are exerted far away from the end-effector, e.g. close to the base link, then the perceived impedance behavior will be different. In that case, an additional contact point estimation would be required for adapting the admittance controller to the current contact point.

If we replace the joint torques by a generalized Cartesian force $\boldsymbol{F} = \boldsymbol{J}^{-T}(\boldsymbol{q})\boldsymbol{\tau}$, the model (4) can be written in Cartesian coordinates as [2]

$$\boldsymbol{\Lambda}(\boldsymbol{q})\ddot{\boldsymbol{x}} + \boldsymbol{\mu}(\boldsymbol{q}, \dot{\boldsymbol{q}})\dot{\boldsymbol{x}} + \boldsymbol{p}(\boldsymbol{q}) = \boldsymbol{F} + \boldsymbol{F}_{\text{ext,c}} \ , \quad (17)$$

where $\boldsymbol{\Lambda}(\boldsymbol{q})$ denotes the Cartesian inertia matrix $\boldsymbol{\Lambda}(\boldsymbol{q}) = (\boldsymbol{J}(\boldsymbol{q})\boldsymbol{M}^{-1}(\boldsymbol{q})\boldsymbol{J}^T(\boldsymbol{q}))^{-1}$ and the matrices $\boldsymbol{\mu}(\boldsymbol{q}, \dot{\boldsymbol{q}})$ and the Cartesian gravity term $\boldsymbol{p}(\boldsymbol{q})$ are given by $\boldsymbol{\mu}(\boldsymbol{q}, \dot{\boldsymbol{q}}) = \boldsymbol{J}^{-T}(\boldsymbol{q})(\boldsymbol{C}(\boldsymbol{q}, \dot{\boldsymbol{q}}) - \boldsymbol{M}(\boldsymbol{q})\boldsymbol{J}^{-1}(\boldsymbol{q})\dot{\boldsymbol{J}}(\boldsymbol{q}))\boldsymbol{J}^{-1}(\boldsymbol{q})$ and $\boldsymbol{p}(\boldsymbol{q}) = \boldsymbol{J}^{-T}(\boldsymbol{q})\boldsymbol{g}(\boldsymbol{q})$, respectively.

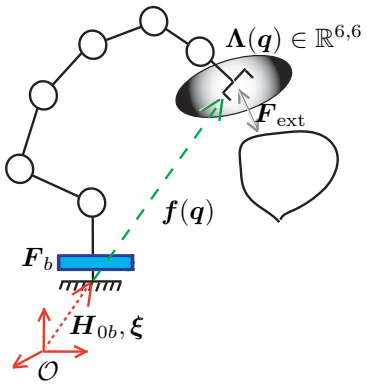

Fig. 4. Operational space model of a robot manipulator mounted on a base FTS.

The relation between the base force and the accelerations, i.e. (5), becomes

$$\boldsymbol{F}_b = \boldsymbol{J}_b^T(\boldsymbol{q})\boldsymbol{F}_{\text{ext,c}} - \boldsymbol{\Lambda}_c(\boldsymbol{q})\ddot{\boldsymbol{x}} - \boldsymbol{\mu}_1(\boldsymbol{q}, \dot{\boldsymbol{q}})\dot{\boldsymbol{x}} - \boldsymbol{g}_b(\boldsymbol{q}) \ , \quad (18)$$

where the inertia coupling matrix $\boldsymbol{\Lambda}_c(\boldsymbol{q})$ and $\boldsymbol{\mu}_1(\boldsymbol{q}, \dot{\boldsymbol{q}})$ are given by $\boldsymbol{\Lambda}_c(\boldsymbol{q}) = \boldsymbol{M}_c(\boldsymbol{q})\boldsymbol{J}^{-1}(\boldsymbol{q})$ and $\boldsymbol{\mu}_1(\boldsymbol{q}, \dot{\boldsymbol{q}}) = (\boldsymbol{C}_1(\boldsymbol{q}, \dot{\boldsymbol{q}}) - \boldsymbol{M}_c(\boldsymbol{q})\boldsymbol{J}^{-1}(\boldsymbol{q})\dot{\boldsymbol{J}}(\boldsymbol{q}))\boldsymbol{J}^{-1}(\boldsymbol{q})$, respectively.

Finally, equation (6) takes the form

$$\boldsymbol{F}_b = \boldsymbol{\Phi}^{\Lambda+}(\boldsymbol{q}) \left(\begin{bmatrix} \boldsymbol{J}_b^T(\boldsymbol{q}) \\ \boldsymbol{I} \end{bmatrix} \boldsymbol{F}_{\text{ext,c}} + \begin{pmatrix} \boldsymbol{0} \\ \boldsymbol{F} \end{pmatrix} - \begin{bmatrix} \boldsymbol{\mu}_1(\boldsymbol{q}, \dot{\boldsymbol{q}})\dot{\boldsymbol{x}} + \boldsymbol{g}_b(\boldsymbol{q}) \\ \boldsymbol{\mu}(\boldsymbol{q}, \dot{\boldsymbol{q}})\dot{\boldsymbol{x}} + \boldsymbol{p}(\boldsymbol{q}) \end{bmatrix} \right) \ , \quad (19)$$

where the matrix $\boldsymbol{\Phi}^{\Lambda+}(\boldsymbol{q})$ is given by

$$\boldsymbol{\Phi}^{\Lambda+}(\boldsymbol{q}) = \begin{bmatrix} \boldsymbol{I} & -\boldsymbol{M}_c(\boldsymbol{q})\boldsymbol{M}^{-1}(\boldsymbol{q})\boldsymbol{J}^T(\boldsymbol{q}) \end{bmatrix} \ .$$

Equation (15) defines an impedance relation $\Im(\dot{\boldsymbol{x}}, \boldsymbol{F}_{\text{ext,c}})$ between the Cartesian velocity and the generalized external forces. In order to transform it into an impedance relation $\Im^*(\dot{\boldsymbol{x}}, \boldsymbol{F}_b)$ between the velocity and the generalized base force, we utilize (18) to obtain

$$\left(\boldsymbol{\Lambda}_d - \boldsymbol{J}_b^{-T}(\boldsymbol{q})\boldsymbol{\Lambda}_c(\boldsymbol{q})\right)\ddot{\boldsymbol{x}} + \left(\boldsymbol{D}_d - \boldsymbol{J}_b^{-T}(\boldsymbol{q})\boldsymbol{\mu}_1(\boldsymbol{q}, \dot{\boldsymbol{q}})\right)\dot{\boldsymbol{x}} + \boldsymbol{K}_d(\boldsymbol{x} - \boldsymbol{x}_d) = \boldsymbol{J}_b^{-T}(\boldsymbol{F}_b + \boldsymbol{g}_b(\boldsymbol{q})) \ . \quad (20)$$

Equation (20) presents the main component of our proposed controller design. Similar to the case of the one-DOF system in Sec. 3, we utilize (20) for designing an admittance controller with underlying position controller. Instead of implementing the underlying position controller based on the Cartesian dynamics (17), a joint level position controller can be used and combined with the Cartesian admittance by inverse kinematics as shown in Fig. 5.

[2] While the assumptions made in this section would formally allow to represent the system dynamics in terms of $\boldsymbol{x} = \boldsymbol{f}^{-1}(\boldsymbol{q})$ and $\dot{\boldsymbol{x}}$ only, we keep the dependence of the dynamic equations on the joint angles $\boldsymbol{q}$ since this formulation is much closer to the actual implementation of the control law.

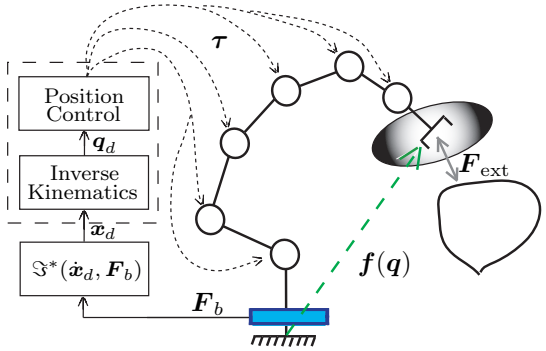

Fig. 5. Cartesian admittance control of a manipulator mounted on a base FTS.

5. SIMULATION RESULTS

In this section, we verify the control approach from Fig. 5 by simulation of a planar robot model with three DOF. The model is shown in Fig. 6. For the inner loop joint position controller, we use a PD-like controller with a diagonal matrix for the proportional gain matrix. The used proportional gains are given in Tab. 1. For the design of the derivative gain matrix we use the double diagonalization method of [17] with an overall damping factor of 0.7.

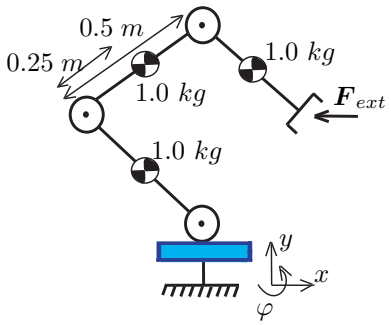

Fig. 6. Simulation model: A planar three-DOF manipulator mounted on a base FTS. The link length of all three segments is set to 0.5m. The inertia of the links is represented by a single mass located in the center of the link segments. The external force acts in the horizontal x-direction. As Cartesian coordinates, the end-effector position (x, y) and orientation ϕ are used.

Table 1. Gains of the joint position controller

Joint	1	2	3
Prop. Gain	5 10^3 Nm/rad	5 10^3 Nm/rad	10^3 Nm/rad

Table 2. Impedance Parameters

Direction	x	y	φ
Inertia	5 Ns^2/m	5 Ns^2/m	5 Nms^2/rad
Stiffness	10 N/m	10 N/m	1 Nm/rad
Damping	9.9 Ns/m	9.9 Ns/m	3.1305 Nms/rad

The desired impedance is given by (15), where the inertia, damping, and stiffness matrix are chosen as diagonal matrices with the diagonal elements according to Tab. 2. For the outer loop admittance controller, we compare two different controllers. First, we observe the closed loop behavior with an admittance controller in which the components $-\boldsymbol{J}_b^{-T}(\boldsymbol{q})\boldsymbol{\Lambda}_c(\boldsymbol{q})$ and $-\boldsymbol{J}_b^{-T}(\boldsymbol{q})\boldsymbol{\mu}_1(\boldsymbol{q}, \dot{\boldsymbol{q}})$ from (20) are neglected. This situation corresponds to neglecting the fact that the base FTS measures the dynamic effects of the robot's motion. As a second controller, we use the complete equation (20) in the admittance part.

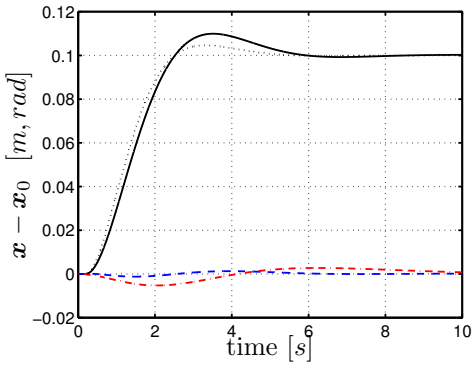

Fig. 7. Simulation result with an admittance controller in which the inertia coupling matrix $\boldsymbol{\Lambda}_c(\boldsymbol{q})$ is neglected. The desired step response in x-direction is given by the black dotted line. The simulation result for the Cartesian motion in x-, y-, and ϕ-direction are shown by the black solid line, the blue dashed line and the red dashed-dotted line, respectively.

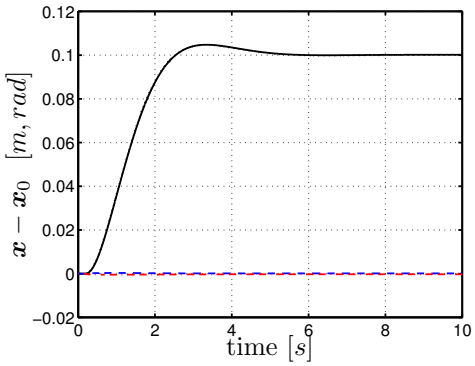

Fig. 8. Simulation result with the admittance controller based on (20). The desired step response in x-direction is given by the black dotted line (difficult to see in this plot). The simulation result for the Cartesian motion in x-, y-, and ϕ-direction are shown by the black solid line, the blue dashed line and the red dashed-dotted line, respectively.

We simulate a step response for the external force in x-direction changing from zero to 1 N with the starting configuration shown in Fig. 6. Figure 7 shows the simulation result for the controller in which the inertia coupling matrix is neglected. The desired step response in x-direction according to the parameters in Tab. 2 is shown by the black dotted line, while the simulation result is shown by the black solid line. For this case, one can see a clear mismatch between the actual and the desired behavior. This can also be seen by observing the motion in y- and ϕ-direction, which should remain zero according to the desired behavior. On the other hand, the result with the admittance controller based on (20) is shown in Fig. 8. One can see that the step response corresponds much better to the desired behavior. The remaining motion in y- and ϕ-direction (difficult to see in Fig. 8) is resulting from the dynamics of the inner loop position controller in the admittance setting.

6. SUMMARY AND OUTLOOK

In this paper, the admittance control problem for a position controlled manipulator is analyzed for the situation that the external forces are measured indirectly by a FTS mounted at the robot's base and not at the end-effector. From the analysis of a simple one-DOF model, it becomes clear how the the dynamic forces on the base sensor influence the achievable closed loop dynamics. In the multibody case, a generalization of the one-DOF controller design to a Cartesian admittance controller was discussed, leading to an admittance design based on (20). The effect of the inertia coupling terms in (20) was analyzed in a simple planar simulation study. In the case of a fixed base manipulator, the use of the base sensor has in general the advantage that it allows to perceive forces acting anywhere on the robot's structure. This allows to implement a compliant behavior in which the physical interaction is not restricted to contacts at the end-effector. However, for handling also forces acting "far" away from the end-effector (e.g., close to the base link), an additional contact point estimation would be required for adapting the controller to the current contact point. These types of compliant behaviors, which are insensitive to the precise contact location, can be of use for service robotics applications in human environments where the interaction of the robot with the environment (or with humans) cannot be fully planned in advance. Moreover, we believe that the analysis can also be useful for implementing compliance control of legged robotic systems in which the ground reaction forces of the feet are measured by FTSs.

REFERENCES

[1] N. Hogan, "Impedance control: An approach to manipulation, part I - theory," *ASME Journal of Dynamic Systems, Measurement, and Control*, vol. 107, pp. 1–7, 1985.

[2] J. Luh, W. Fisher, and R. Paul, "Joint torque control by a direct feedback for industrial robots," *IEEE Transactions on Automatic Control*, vol. 28, no. 2, pp. 153–161, 1983.

[3] G. Hirzinger, A. Albu-Schäffer, M. Hähnle, I. Schaefer, and N. Sporer, "On a new generation of torque controlled light-weight robots." in *IEEE Int. Conf. on Robotics and Automation*, 2001, pp. 3356–3363.

[4] G. Hirzinger, N. Sporer, A. Albu-Schäffer, M. Hähnle, R. Krenn, A. Pascucci, and M. Schedl, "DLR's torque-controlled light weight robot III - are we reaching the technological limits now?" in *IEEE Int. Conf. on Robotics and Automation*, 2002, pp. 1710–1716.

[5] B. Siciliano, L. Sciavicco, L. Villani, and G. Oriolo, *Robotics: Modelling, Planning and Control*, ser. Advanced Textbooks in Control and Signal Processing. Springer-Verlag, 2009.

[6] M. Lee and H. Nicholls, "Tactile sensing for mechatronics: a state of the art survey," *Mechatronics*, vol. 9, no. 1, pp. 1–31, 1999.

[7] Ch. Ott, O. Eiberger, W. Friedl, B. Bäuml, U. Hillenbrand, Ch. Borst, A. Albu-Schäffer, B. Brunner, H. Hirschmüller, S. Kielhöfer, R. Konietschke, M. Suppa, T. Wimböck, F. Zacharias, and G. Hirzinger, "A humanoid two-arm system for dexterous manipulation," in *IEEE-RAS International Conference on Humanoid Robots*, 2006, pp. 276–283.

[8] G. Cheng, S.-H. Hyon, J. Morimoto, A. Ude, G. Colvin, W. Scroggin, and S. Jacobsen, "Cb: A humanoid research platform for exploring neuroscience," in *IEEE-RAS International Conference on Humanoid Robots*, 2006, pp. 182–187.

[9] S. Kajita, *Humanoid Robot.* Ohmsha, 2005, (in Japanese).

[10] H. West, E. Papadopoulos, S. Dubowsky, and H. Cheah, "A method for estimating the mass properties of a manipulator by measuring the reaction moments at its base," in *IEEE Int. Conf. on Robotics and Automation*, 1989, pp. 1510–1516.

[11] G. Liu, K. Iagnemma, S. Dubowsky, and G. Morel, "A base force/torque sensor approach to robot manipulator inertial parameter estimation," in *IEEE Int. Conf. on Robotics and Automation*, 1998, pp. 3316–3321.

[12] G. Morel, K. Iagnemma, and S. Dubowsky, "The precise control of manipulators with high joint-friction using base force/torque sensing," *Automatica*, vol. 36, no. 7, pp. 931–941, 2000.

[13] J. de Jalon and E. Bayo, *Kinematic and Dynamic Simulation of Multibody Systems: The Real-Time Challenge*, ser. Mechanical Engineering Series. Springer-Verlag, 1994.

[14] R. Murray, Z. Li, and S. Sastry, *A Mathematical Introduction to Robotic Manipulation.* CRC Press, 1994.

[15] J. Park, W. Chung, and Y. Youm, "On dynamical decoupling of kinematically redundant manipulators," in *IEEE/RSJ Int. Conf. on Intelligent Robots and Systems*, 1999, pp. 1495–1500.

[16] Ch. Ott, A. Kugi, and Y. Nakamura, "Resolving the problem of non-integrability of nullspace velocities for compliance control of redundant manipulators by using semi-definite lyapunov functions," in *ICRA*, 2008, pp. 1999–2004.

[17] A. Albu-Schäffer, Ch. Ott, U. Frese, and G. Hirzinger, "Cartesian impedance control of redundant robots: Recent results with the dlr-light-weight-arms," in *IEEE Int. Conf. on Robotics and Automation*, 2003, pp. 3704–3709.

Appendix A. DERIVATION OF $\boldsymbol{\Phi}^{M+}$

In this appendix we show that the matrix $\boldsymbol{\Phi}^{M+}(\boldsymbol{q})$ is given by $\boldsymbol{\Phi}^{M+}(\boldsymbol{q}) = \begin{bmatrix}\boldsymbol{I} & -\boldsymbol{M}_c(\boldsymbol{q})\boldsymbol{M}^{-1}(\boldsymbol{q})\end{bmatrix}$. Therefore, let us write it first in the general form $\boldsymbol{\Phi}^{M+}(\boldsymbol{q}) = [\boldsymbol{B}_l(\boldsymbol{q})\ \boldsymbol{B}_r(\boldsymbol{q})]$ with some matrices $\boldsymbol{B}_l(\boldsymbol{q}) \in \mathbb{R}^{6\times 6}$ and $\boldsymbol{B}_r(\boldsymbol{q}) \in \mathbb{R}^{6\times n}$.

Consider the steady state with $\ddot{\boldsymbol{q}} = \dot{\boldsymbol{q}} = \boldsymbol{0}$. Since (4)-(6) hold in any case, they must also hold in steady state. From (4), one can see that in steady state the joint torque must be equal to $\boldsymbol{\tau} = -\boldsymbol{\tau}_{\text{ext,m}} + \boldsymbol{g}(\boldsymbol{q})$, such that equation (6) becomes $\boldsymbol{F}_b = \boldsymbol{B}_l(\boldsymbol{q})(\boldsymbol{\tau}_{\text{ext,b}} - \boldsymbol{g}_b(\boldsymbol{q}))$. Since in steady state $\boldsymbol{F}_b$ must be equal to the the sum of the robot's weight $-\boldsymbol{g}_b(\boldsymbol{q})$ plus the effect of the external forces onto the base, one can see that $\boldsymbol{B}_l(\boldsymbol{q})$ must be equal to $\boldsymbol{B}_l = \boldsymbol{I}$.

Further, by substituting the torque from (4) into (6) and utilizing the result $\boldsymbol{B}_l = \boldsymbol{I}$, we obtain

$$\boldsymbol{F}_b = [\boldsymbol{I}\ \boldsymbol{B}_r(\boldsymbol{q})] \begin{pmatrix} \boldsymbol{\tau}_{\text{ext,b}} - \boldsymbol{C}_1(\boldsymbol{q},\dot{\boldsymbol{q}})\dot{\boldsymbol{q}} - \boldsymbol{g}_b(\boldsymbol{q}) \\ \boldsymbol{M}(\boldsymbol{q})\ddot{\boldsymbol{q}} \end{pmatrix} .$$

By comparing this equation with (5), one can see that $\boldsymbol{B}_r(\boldsymbol{q})$ must be given by $\boldsymbol{B}_r(\boldsymbol{q}) = -\boldsymbol{M}_c(\boldsymbol{q})\boldsymbol{M}^{-1}(\boldsymbol{q})$.